

2

OFFICE OF NAVAL RESEARCH

Grant No. N00014-90-J-1263

RCT Project 4133002---05

Technical Report #4

**IN-SITU SURFACE X-RAY SCATTERING MEASUREMENTS OF  
ELECTROCHEMICALLY DEPOSITED BISMUTH ON SILVER (III):  
STRUCTURE, COMPRESSIBILITY, AND COMPARISON WITH EX-SITU  
LEED MEASUREMENTS**

by

Michael F. Toney\*, Joseph G. Gordon\*, Mahesh G. Samant\*,  
Gary L. Borges\*, David G. Wiesler\*, Dennis Yee\*\* and  
Larry B. Sorensen\*\*

Prepared for Publication in the  
Physical Review B

\*IMB Research Division  
Almaden Research Center  
650 Harry Road  
San José, California 95120-6099

\*\*Department of Physics FM-15  
University of Washington  
Seattle, WA 98195

DTIC  
ELECTE  
S B D  
MAR 6 1991

Reproduction in whole or in part is permitted  
for any purpose of the United States Government

\*This document has been approved for public release  
and sale; its distribution is unlimited

\*This statement should also appear in Item 10 of Document Control Data  
- DD Form 1473. Copies of form available from cognizant contract  
administrator.

AD-A232 624

91 3 04 025

## REPORT DOCUMENTATION PAGE

1a. REPORT SECURITY CLASSIFICATION		1b. RESTRICTIVE MARKINGS	
2a. SECURITY CLASSIFICATION AUTHORITY		3. DISTRIBUTION / AVAILABILITY OF REPORT	
2b. DECLASSIFICATION / DOWNGRADING SCHEDULE			
4. PERFORMING ORGANIZATION REPORT NUMBER(S) Technical Report #4		5. MONITORING ORGANIZATION REPORT NUMBER(S)	
6a. NAME OF PERFORMING ORGANIZATION Physics Department University of Puerto Rico	6b. OFFICE SYMBOL (If applicable)	7a. NAME OF MONITORING ORGANIZATION	
6c. ADDRESS (City, State, and ZIP Code) Río Piedras, P.R. 00931-3343		7b. ADDRESS (City, State, and ZIP Code)	
8a. NAME OF FUNDING / SPONSORING ORGANIZATION Chemistry Office of Naval Research	8b. OFFICE SYMBOL (If applicable) Code 472	9. PROCUREMENT INSTRUMENT IDENTIFICATION NUMBER RCT Project 4133002---05	
8c. ADDRESS (City, State, and ZIP Code) Arlington Virginia 22217-5000		10. SOURCE OF FUNDING NUMBERS	
		PROGRAM ELEMENT NO.	PROJECT NO.
		TASK NO.	WORK UNIT ACCESSION NO.
11. TITLE (Include Security Classification) IN-SITU SURFACE X-RAY SCATTERING MEASUREMENTS OF ELECTROCHEMICALLY DEPOSITED BISMUTH ON SILVER (111): STRUCTURE, COMPRESSIBILITY, AND COMPARISON WITH EX-SITU LEED MEASUREMENTS			
12. PERSONAL AUTHOR(S) M.F. Toney, J.G. Gordon, M.G. Samant, G.L. Borges, P.G. Wiesler, D.Yee and L.B. Sorensen			
13a. TYPE OF REPORT Summary	13b. TIME COVERED FROM _____ TO _____	14. DATE OF REPORT (Year, Month, Day) 1-29-91	15. PAGE COUNT 29
16. SUPPLEMENTARY NOTATION			
17. COSATI CODES		18. SUBJECT TERMS (Continue on reverse if necessary and identify by block number)	
FIELD	GROUP		
19. ABSTRACT (Continue on reverse if necessary and identify by block number)			
<p>We report in-situ surface X-ray scattering measurements of the structure and compressibility of electrochemically deposited Bi monolayers on Ag(III) and compare the in-situ structure with results from previous ex-situ experiments on emersed electrodes, where the structure was studied with low-energy electron diffraction (LEED). We find that the Bi monolayer forms an unusual structure: a two-dimensional rectangular lattice that is uniaxially commensurate with the hexagonal Ag(III) surface along the Ag[<math>\bar{2}11</math>] direction. There are two Bi adatoms per rectangular unit cell and one adatom is displaced from the centered-rectangular position by <math>\approx 0.25\text{\AA}</math> along the commensurate direction. The displacement shortens two of the Bi-Bi</p>			
20. DISTRIBUTION / AVAILABILITY OF ABSTRACT <input checked="" type="checkbox"/> UNCLASSIFIED/UNLIMITED <input type="checkbox"/> SAME AS RPT <input type="checkbox"/> DTIC USERS		21. ABSTRACT SECURITY CLASSIFICATION	
22a. NAME OF RESPONSIBLE INDIVIDUAL Dr. Robert J. Nowak		22b. TELEPHONE (Include Area Code) (202) 696-4410	22c. OFFICE SYMBOL ONR 472

near-neighbor bond distances but lengthens two others and may reflect the tendency toward covalent bonding in Bi. With increasing coverage (decreasing applied potential), the Bi monolayer compresses uniaxially along the incommensurate direction ( $\text{Ag}[011]$ ), which preserves the uniaxially commensurate structure. The measured two-dimensional compressibility,  $k_{2d} = 0.75 \text{ \AA}^2/\text{eV}$ , is similar to the previously measured compressibilities of TI and Pb monolayers on  $\text{Ag}(\text{III})$  and  $\text{Au}(\text{III})$  and is in reasonable agreement with theoretical estimates. The presence or absence of CI ions does not affect the structure or its compressibility. Although the in-situ rectangular structure differs from that proposed in the ex-situ LEED experiments of Languren-Davidson et al. (Langmuir 4,224 (1988)), we believe that the in-situ and ex-situ structures are in fact the same. We show that our proposed rectangular structure completely explains the LEED data, when multiple scattering (typically present in Leed) is taken into account; in contrast, the complicated  $2 \sqrt{3} \times 2 \sqrt{3} - \text{R}30$  structure proposed from LEED is inconsistent with our in-situ data. This comparison demonstrates that, at least for the case of  $\text{Bi}/\text{Ag}(\text{III})$ , the ex-situ emersion experiments preserve the in-situ monolayer structure.



Accession For	
NTIS GRA&I	<input checked="" type="checkbox"/>
DTIC TAB	<input type="checkbox"/>
Unannounced	<input type="checkbox"/>
Justification	
By	
Distribution/	
Availability Codes	
Dist	Avail and/or Special
A-1	

# Research Report

## IN-SITU SURFACE X-RAY SCATTERING MEASUREMENTS OF ELECTROCHEMICALLY DEPOSITED BISMUTH ON SILVER (111): STRUCTURE, COMPRESSIBILITY, AND COMPARISON WITH EX-SITU LEED MEASUREMENTS

M. F. Toney  
M. G. Samant  
D. G. Wiesler  
J. G. Gordon  
G. L. Borges  
D. Yee\*  
L. B. Sorensen\*

IBM Research Division  
Almaden Research Center  
650 Harry Road  
San Jose, California 95120-6099

\*Department of Physics FM-15  
University of Washington  
Seattle, Washington 98195

### LIMITED DISTRIBUTION NOTICE

This report has been submitted for publication outside of IBM and will probably be copyrighted if accepted for publication. It has been issued as a Research Report for early dissemination of its contents. In view of the transfer of copyright to the outside publisher, its distribution outside of IBM prior to publication should be limited to peer communications and specific requests. After outside publication, requests should be filled only by reprints or legally obtained copies of the article (e.g., payment of royalties).



Research Division

Yorktown Heights, New York • San Jose, California • Zurich, Switzerland

## **In-situ Surface X-ray Scattering Measurements of Electrochemically Deposited Bi on Ag(111): Structure, Compressibility, and Comparison with Ex-Situ LEED Measurements**

Michael F. Toney, Joseph G. Gordon, Mahesh G. Samant, Gary L. Borges, David G. Wiesler  
IBM Research Division  
Almaden Research Center  
650 Harry Road  
San Jose, California 95120-6099

Dennis Yee and Larry B. Sorensen  
Department of Physics FM-15  
University of Washington  
Seattle, WA 98195

### ***Abstract***

We report in-situ surface x-ray scattering measurements of the structure and compressibility of electrochemically deposited Bi monolayers on Ag(111) and compare the in-situ structure with results from previous ex-situ experiments on emersed electrodes, where the structure was studied with low-energy electron diffraction (LEED). We find that the Bi monolayer forms an unusual structure: a two-dimensional *rectangular* lattice that is uniaxially commensurate with the *hexagonal* Ag(111) surface along the Ag  $[\bar{2}11]$  direction. There are two Bi adatoms per rectangular unit cell and one adatom is displaced from the centered-rectangular position by  $\approx 0.25\text{\AA}$  along the commensurate direction. The displacement shortens two of the Bi-Bi near-neighbor bond distances but lengthens two others and may reflect the tendency toward covalent bonding in Bi. With increasing coverage (decreasing applied potential), the Bi monolayer compresses uniaxially along the incommensurate direction (Ag  $[01\bar{1}]$ ), which preserves the uniaxially commensurate structure. The measured two-dimensional compressibility,  $\kappa_{2D} = 0.75\text{\AA}^2/\text{eV}$ , is similar to the previously measured compressibilities of Tl and Pb monolayers on Ag(111) and Au(111) and is in reasonable agreement with theoretical estimates. The presence or absence of  $\text{Cl}^-$  ions does not affect the structure or its compressibility. Although the in-situ rectangular structure differs from that proposed

in the ex-situ LEED experiments of Laguren-Davidson et al. (Langmuir 4, 224 (1988)), we believe that the in-situ and ex-situ structures are in fact the same. We show that our proposed rectangular structure completely explains the LEED data, when multiple scattering (typically present in LEED) is taken into account; in contrast, the complicated  $2\sqrt{3} \times 2\sqrt{3} - R30^\circ$  structure proposed from LEED is inconsistent with our in-situ data. This comparison demonstrates that, at least for the case of Bi/Ag(111), the ex-situ emission experiments preserve the in-situ monolayer structure.

## *1. Introduction*

The atomic structure at solid-liquid interfaces is of fundamental importance in electrochemistry, since this structure strongly affects the chemical and physical properties of the interface. Consequently, considerable effort has been directed toward studying this interface and adsorbed layers at the interface using traditional electrochemical and spectroscopic techniques. However, these techniques only provide indirect information about the atomic scale structure of the interface. To obtain more direct information, many investigators have adopted the use of ex-situ techniques, where the electrode surface is examined with surface science methods following emersion of the electrode and transfer into ultrahigh vacuum (UIHV).<sup>1-5</sup> These emersion experiments have provided valuable information on the ex-situ structure of layers adsorbed from solution. However, the question of whether the ex-situ structure determined in the emersion experiments is the same as the in-situ structure remains open; the removal of the solvent and the loss of potential control can cause the surface to rearrange during the emersion process. Thus, it is very important to determine the in-situ structure of layers adsorbed at solid-liquid interfaces and to compare these in-situ structures with those measured ex-situ. This will permit an understanding of the extent to which these ex-situ experiments preserve the in-situ structure.

As we have discussed and shown before, surface x-ray diffraction and x-ray spectroscopies are well suited to in-situ measurements of atomic arrangements at the solid-liquid interface.<sup>6-10</sup> The weakly interacting nature of hard x-ray radiation enables x-rays to penetrate the electrolyte and directly probe the interface. In addition, the high x-ray flux available from modern synchrotron radiation sources permits surface diffraction measurements from single adsorbed layers with count rates of up to 30,000 counts per second. Because of the weak interaction between x-rays and matter, a simple kinematic (or single scattering) approach can be used to analyze experimental data and determine the surface structure. This simple analysis is one of the most important advantages of surface x-ray diffraction compared to the most common surface structural

technique. low-energy electron diffraction (LEED), where multiple scattering of electrons *must* be taken into account.

In this paper, we report a surface x-ray diffraction study of the in-situ structure of electrochemically deposited monolayers of Bi on Ag(111), making use of the simplified kinematic interpretation of x-ray diffraction patterns. We find that Bi forms a rectangular lattice that has two Bi atoms per unit cell; the lattice is uniaxially commensurate with the hexagonal Ag(111) surface along the Ag  $[\bar{2}11]$  direction and has incommensurate Bi rows along the Ag  $[01\bar{1}]$  direction. With increasing coverage, the Bi monolayer remains commensurate with the Ag surface along the Ag  $[\bar{2}11]$  direction, but compresses uniaxially along Ag  $[01\bar{1}]$ . The coverage was varied by changing the applied potential, and from these measurements, the two-dimensional compressibility is determined to be  $\kappa_{2D} = 0.75 \text{ \AA}^2/\text{eV}$ . We compare the in-situ structure to that proposed in the ex-situ experiments of Laguren-Davidson et al.<sup>5</sup> (LLSH), who used the emersion technique and characterized the structure of Bi/Ag(111) with LEED. Although the in-situ rectangular structure is different from the  $2\sqrt{3} \times 2\sqrt{3} - R30^\circ$  structure proposed by LLSH,<sup>5</sup> we believe the in-situ and ex-situ structures to be the same. We show that when multiple scattering is included, the in-situ rectangular structure reproduces the observed LEED pattern,<sup>5</sup> while the  $2\sqrt{3} \times 2\sqrt{3} - R30^\circ$  structure is inconsistent with our data. This particular case illustrates the importance and utility of in-situ surface diffraction measurements of the electrochemical interface.

## ***II. Experimental Aspects***

The x-ray data were collected at the National Synchrotron Light Source beam line X20C.<sup>11, 12</sup> An incident x-ray energy of 10005 eV ( $1.2395 \text{ \AA}$ ) was selected using a Si(111) double monochromator. The x-rays were focused with a grazing incidence mirror; at the sample, this produced vertical and horizontal full-widths at half-maximum (FWHM) of 0.8mm and 0.9mm, respectively. The incident beam intensity was monitored by a NaI scintillation detector viewing a thin Kapton foil. The diffracted beam was analyzed with



1mrad Soller slits and the intensity was measured with a NaI scintillation detector. The sample was aligned using the bulk Ag reflections and all data were collected in the symmetric ( $\omega = 0$ ) mode.<sup>13</sup>

Our experiments were all performed in-situ (in electrolyte), under potential control, and at room temperature. The electrochemical cell is the same as that used in our earlier investigations.<sup>7, 8, 14</sup> The electrode substrates were epitaxially grown thin films of Ag that were vapor deposited onto freshly cleaved mica.<sup>7, 8</sup> The Bi monolayer was electrochemically deposited with the cell inflated so a relatively thick ( $\sim 1\text{mm}$ ) layer of electrolyte covers the electrode. The electrolyte was then partially removed and the surface diffraction data were measured through the thin ( $\lesssim 30\mu\text{m}$ ) layer of electrolyte that remained above the electrode. Since the cyclic voltammograms for the deposition of Bi are sensitive to the presence of  $\text{Cl}^-$ , we investigated the possible effects of  $\text{Cl}^-$  ions on the structure and compressibility of the Bi monolayer. Two different electrolytes were used: a chloride-containing solution of 0.1M  $\text{HClO}_4$  with 2.5mM  $\text{Bi}_2\text{O}_3$  and 0.35mM  $\text{NaCl}$ , and a chloride-free solution of 0.1M  $\text{HClO}_4$  containing 2.5mM  $\text{Bi}_2\text{O}_3$ . All potentials were measured relative to the Ag/AgCl (3M KCl) reference electrode in the diffraction cell. For the experiments in the chloride-containing electrolyte, the Ag/AgCl reference electrode was isolated from the cell by a single porous frit, but to prevent contamination during the experiments in the chloride-free electrolyte, the reference electrode was isolated behind a second porous junction filled with 0.1M  $\text{HClO}_4$ .

The electrochemical deposition of Bi on Ag(111) occurs in two distinct stages. First, at an electrode potential positive of the thermodynamic (Nernst) potential for bulk deposition, a single monolayer is deposited,<sup>15, 16</sup> and then at the Nernst potential, bulk Bi is deposited. The monolayer deposition process is referred to as underpotential deposition (UPD), and on single crystals, UPD deposits often form well defined, ordered monolayers.<sup>7, 8, 14, 17, 18</sup> The measured cyclic voltammograms for Bi deposition on Ag(111) from chloride-free and chloride-containing electrolytes are shown in Figures 1(a) and (b), respectively. Our x-ray data show that the large peak at approximately

110mV corresponds to the deposition of a Bi monolayer. The stripping peak is noticeably broader, which is due to slow kinetics; in addition, slow kinetics probably affect the shape and position of the deposition peak.<sup>15</sup> The charge passed during deposition is 450-480  $\mu\text{C}/\text{cm}^2$ , consistent with previous measurements (450-470  $\mu\text{C}/\text{cm}^2$ ).<sup>15, 16</sup>

The Ag substrates used in our experiments are of high quality and have large, flat (111) faces that are defect free. This high quality is shown by the cyclic voltammograms, which agree with those published on single-crystals,<sup>15, 16</sup> and by the intense, sharp surface diffraction peaks from the Ag substrate. From the width of these surface peaks, we calculate a surface domain size of 500Å and an in-plane mosaic spread of 0.2°.

### *III. In-Situ X-ray Scattering Measurements of the Structure and Compressibility*

The in-situ diffraction pattern for Bi/Ag(111) in the chloride-containing electrolyte is shown in Figure 2. For simplicity, Figure 2(a) shows the pattern that would be observed from a single domain of the rectangular structure. The approximate observed intensity for each diffraction peak is indicated by the size of the filled circles. These intensities are only approximate, since we have not yet made careful crystallographic measurements of the integrated peak intensities. The (03) peak (indicated by the cross) was too weak to be measured and the (01) peak (indicated by the open squares) was obscured by a strong diffraction peak from the mica substrate. Notice that the Bi (20) peak occurs at exactly the same position as the Ag  $\frac{1}{3}(4\bar{2}2)$  surface rod,<sup>6,8, 19</sup> which shows that the rectangular Bi monolayer is commensurate with the Ag substrate in this direction. Because of the three-fold symmetry of the Ag (111) substrate, there are three domains of the rectangular structure, which are commensurate along directions that are rotated 120° and 240° with respect to the domain shown in Figure 2(a). The surface diffraction pattern that we observe is the superposition of all three domains with equal intensity and is shown in Figure 2(b).

Figure 3 shows diffraction scans through the Bi (11), (31), (30), and (03) peaks. In these '*h* scans', the magnitude of the scattering vector is varied, while the component of the scattering vector perpendicular to the surface and the direction of the component parallel to the surface are both fixed.<sup>6</sup> (An illustration of an *h* scan is given in Figure 2.) The (11) peak is very intense compared to the (30) and (31) peaks, which likely reflects a large Debye-Waller factor. The Bi(03) peak was not observed and an *h* scan through the expected position for this peak is shown in Figure 3(d). The open circles are data taken with the Bi monolayer adsorbed on the surface (*V* = 60mV), while the line is data taken at *V* = 250mV, where the Bi monolayer is not adsorbed. The difference between these two (Bi on minus Bi off) is shown in the inset and the arrow marks the expected position of (03) peak. These data show that the Bi(03) peak is absent at the level of the current measurement ( $0.5 \times 10^{-3}$  counts/monitor or 0.1% of the (11) peak intensity). The small intensity offset seen in the inset in Figure 3(d) is due to a slight variation in electrolyte thickness between scans.

The in-situ structure of the Bi monolayer that we deduce from these data is shown in Figure 4. For clarity, we have drawn the Bi[10] rows atop the Ag [01 $\bar{1}$ ] rows, although it is not possible to determine the epitaxy from our current measurements. The rectangular symmetry of the Bi diffraction pattern shows that the monolayer structure is also rectangular. Because the Bi (20) diffraction peak is found at the same position as the Ag  $\frac{1}{3}(4\bar{2}2)$  surface rod, the Bi monolayer is commensurate with the Ag substrate in this direction. The observation of the Bi (30), (10) and (12) diffraction peaks with nonzero intensity means that the monolayer does not have a centered rectangular lattice, but that the adatom near the center of the rectangle is displaced from a perfect centered position along the Bi[10] direction (see Figure 4). Since the (03) peak is *not* observed, there is *no* displacement of the nearly centered adatom along the Bi[01] direction (i.e. the commensurate direction). Note that the displacement along only the Bi[10] direction results in a glide plane along the Bi[01] direction. Although we have not yet performed careful crystallographic intensity measurements, by comparing intensities of the Bi (30) and (11) peaks we estimate that the displacement from the centered-rectangular

position is  $\approx 0.25\text{\AA}$  along Bi[10]. This distortion shortens two of the Bi-Bi near-neighbor bonds while lengthening two others, and it may reflect the tendency toward covalent bonding in Bi.

Throughout this discussion, we have only considered one domain of the rectangular Bi structure and have assumed that this domain is oriented with the Bi[10] direction along the Ag  $[\bar{2}11]$  direction. Recall that there are three other domains on the surface. These domains will not have this orientation, but will have the Bi[10] direction along the either Ag  $[1\bar{2}1]$  or  $[11\bar{2}]$  directions. We have discussed only the domain with Bi[10] parallel to Ag  $[\bar{2}11]$  for notational convenience and simplicity, and we will continue to only consider this domain.

The atomic density of the Bi monolayer (i.e.,  $2/ab$ ) is  $8.75 - 8.91 \times 10^{14}$  atoms/cm<sup>2</sup>, as calculated from the data in Figures 4 and 5. This corresponds to a coverage (density normalized the Ag atomic density) of  $\theta = 0.633-0.644$ . Assuming the Bi<sup>3+</sup> cations are completely discharged on adsorption, the charge passed to form this layer is 420-428  $\mu\text{C}/\text{cm}^2$ , which agrees well with our measurements of total charge (450-480  $\mu\text{C}/\text{cm}^2$ ) and those reported in the literature (450-470  $\mu\text{C}/\text{cm}^2$ ).<sup>15, 16</sup>

The in-situ structure of Bi/Ag(111) is unusual, since the monolayer adopts a *rectangular* symmetry on a surface with *hexagonal* symmetry. We speculate that this results because of a fortuitously close match between the atomic spacings of the Ag substrate and the (102) planes of bulk hexagonal Bi.<sup>20</sup> We are currently conducting complete crystallographic measurements of the intensities of the Bi and Ag surface diffraction rods to quantify the distortion from a centered-rectangular cell and to determine the epitaxy of the Bi[10] rows relative to the Ag surface (i.e., are the Bi[10] rows directly atop the Ag  $[01\bar{1}]$  rows or in between these rows?)

As shown in Figure 1, the presence of Cl<sup>-</sup> ions affects the shape of the UPD adsorption and desorption peaks for Bi/Ag(111).<sup>15</sup> The sharpening and shift of the peaks

show that  $\text{Cl}^-$  speeds up Bi adsorption and desorption. To determine whether  $\text{Cl}^-$  also affects the structure of the Bi monolayer, we have measured the monolayer structure in a chloride-free electrolyte. No systemic changes were observed between chloride-free and chloride-containing electrolytes. The positions of the Bi surface diffraction peaks were identical and the peak intensities were the same, to within our experimental accuracy ( $\approx 30\%$ ). This clearly demonstrates that in both electrolytes the in-situ structures of the Bi monolayers are the same: a uniaxially commensurate, rectangular lattice with similar distortions from a centered rectangular cell. However, because we have not made accurate measurements of the diffracted intensity in both cases, the possibility that there are subtle differences in the positions of the Bi adatoms within the unit cell, due to adsorption of  $\text{Cl}^-$ , cannot be ruled out. (For example, the distortion from a centered rectangular cell could depend on the concentration of  $\text{Cl}^-$ , or some  $\text{Cl}^-$  may be adsorbed in an ordered fashion on the Bi monolayer).

In our previous experiments with UPD Tl and Pb monolayers on Au(111) and Ag(111) substrates, we found that these incommensurate, hexagonal monolayers compressed isotropically as the applied potential was decreased toward the bulk deposition potential.<sup>9, 21, 22</sup> We find a very different result for Bi/Ag(111): the Bi monolayer compresses *uniaxially* along the incommensurate direction ( $\text{Ag}[01\bar{1}]$ ) as the applied potential decreases. This is demonstrated in Figure 5, where the  $a$  and  $b$  lattice constants of the monolayer are plotted vs potential in both chloride-containing and chloride-free electrolytes. In both electrolytes only the incommensurate lattice constant,  $b$ , depends on the applied potential. The commensurate lattice constant,  $a$ , remains locked to the Ag lattice over the entire potential range where the monolayer is stable. Thus, in both electrolytes, the compression preserves the uniaxially commensurate structure.

The compression of the Bi monolayer with decreasing potential is easily understood. First, consider a UPD monolayer in equilibrium with its cations in solution and at a potential where the monolayer has just formed. Decreasing the applied potential (i.e., lowering the Fermi level), creates a thermodynamic driving force to discharge more

$\text{Bi}^{3+}$  cations and hence to pack more Bi atoms on the Ag surface. The compression is a necessary consequence of the increased packing density. Alternatively, one can consider that as the applied potential decreases, the chemical potential of the adatoms in the monolayer increases, because the potential drop across the metal/solution interface decreases. Since the chemical potential of the monolayer has increased, the monolayer free energy can be reduced by increasing the number of Bi adatoms on the Ag surface. The compression of electrochemically deposited layers is completely analogous to vacuum experiments on the adsorption of rare gases. Since the chemical potential of the adsorbed layer is controlled by the vapor pressure of the gas, an increase in the vapor pressure causes a compression of the adsorbed monolayer.<sup>23-26</sup>

We have previously shown that the change in monolayer area with applied potential can be used to determine the two-dimensional (2D) isothermal compressibility of the monolayer,  $\kappa_{2D}$ , and we have determined  $\kappa_{2D}$  for the incommensurate, hexagonal monolayers of Pb and Tl on Ag(111) and Au(111).<sup>6, 9, 21</sup> By analogy with bulk matter,  $\kappa_{2D}$  is:<sup>27</sup>

$$\kappa_{2D} \equiv -\left(\frac{1}{a}\right)\left(\frac{\partial a}{\partial \phi}\right)_T = -\left(\frac{\partial a}{\partial \mu}\right)_T, \quad (1)$$

where  $\phi$  is the 2D spreading pressure,  $a$  the atomic area, and  $\mu$  the chemical potential of the monolayer. The formal expression of the relationship between chemical potential and applied potential is

$$d\mu = -Ze dV, \quad (2)$$

where  $Z$  is the number of electrons transferred per atom deposited and  $V$  is the applied potential.<sup>17</sup> It is important to note that this relationship requires chemical and thermal equilibrium between the monolayer and the ions in solution. Using Equations (1) and (2) and the slope from Figure 5(b), we calculate  $\kappa_{2D} = 0.75 \text{ \AA}^2/\text{eV}$  for Bi/Ag(111). This is about the same as our previous results for Tl ( $\kappa_{2D} = 1.6\text{-}2.0 \text{ \AA}^2/\text{eV}$ ) and Pb ( $\kappa_{2D} = 1.2\text{-}1.6 \text{ \AA}^2/\text{eV}$ ).<sup>6, 9, 21</sup> It is also in reasonable agreement with  $\kappa_{2D} (\approx 0.2 \text{ \AA}^2/\text{eV})$

calculated for a model of the monolayer compressibility that considers only the electron compressibility and approximates this as  $\kappa_{2D}$  for a 2D free electron gas.<sup>6, 21</sup> We note that although the compression is uniaxial, the compressibility we measure is a *two-dimensional* compressibility, not a one-dimensional compressibility, since the monolayer is inherently two dimensional.

#### *IV. Comparison with Ex-situ LEED Results*

This experiment permits the first direct comparison between an in-situ, solid-liquid interfacial structure and the structure present after emersion in the situation where the surface is not grossly altered due to oxidation on emersion. This comparison is a crucial test of whether the in-situ structure of UPD monolayers is changed during the emersion process and it will help determine the extent to which these ex-situ experiments preserve the in-situ structure. In this case, UPD Bi monolayers maintain the same structure after emersion; in other cases, (e.g., Tl and Pb on Ag(111))<sup>4, 5</sup> the monolayers are substantially altered due to oxidation on emersion.

In their ex-situ study, Laguren-Davidson et al. (LLSH),<sup>5</sup> investigated the electrodeposition of Bi onto a Ag(111) single crystal from an aqueous solution of 0.02M acetic acid, 0.01M trifluoroacetate (TFA), and  $10^{-4}$ M bismuth(III) acetate. The voltammetric behavior in TFA is similar to the behavior we have observed in  $\text{HClO}_4$ . After deposition of a full monolayer of Bi, LLSH removed the electrode from solution while maintaining potential control, evacuated the chamber containing the electrode, and characterized the electrode surface with Auger spectroscopy and LEED.<sup>5</sup> After characterization, the electrode was reimmersed and the open circuit potential was observed to be negative of the Bi UPD peak, indicating the monolayer was stable.<sup>5</sup>

Figure 6(a) shows the LEED pattern for Bi/Ag(111) obtained at normal incidence and for an electron energy of 47eV.<sup>5, 28</sup> The observed Ag diffraction spots are indicated by the open circles and the spot sizes roughly indicate the observed intensities. LLSH

interpreted this pattern purely kinematically (multiple scattering was not considered) and proposed a complicated  $2\sqrt{3} \times 2\sqrt{3} - R30^\circ$  structure with anti-phase domains in the form of strips with an average width of  $8.5\sqrt{3}$  Ag unit cells.<sup>5</sup> The full dynamical LEED analysis necessary to determine the multiple scattering contributions to the observed LEED pattern was not performed. This is a complex procedure, but is often necessary to derive surface structure from LEED. Although the  $2\sqrt{3} \times 2\sqrt{3} - R30^\circ$ , anti-phase domain structure is very different from the uniaxially commensurate rectangular structure determined from our in-situ x-ray results, we show below that the in-situ rectangular structure completely explains the observed LEED pattern (Figure 6(a)), when multiple scattering is considered. Thus, we believe that the Bi monolayer structure observed ex-situ with LEED is the same as the distorted rectangular structure we observe in-situ. (Of course, the size of the distortion in the in-situ and ex-situ systems may be slightly different.)

A comparison of the LEED pattern in Figure 6(a) with the in-plane x-ray diffraction pattern in Figure 2(b) shows that all of the x-ray diffraction peaks are observed in the LEED pattern; however, there are LEED spots that do not appear in the x-ray pattern and these spots are enclosed by the rectangles and triangles in Figure 6(a). Since the x-ray pattern shows all the spots that are kinematically allowed, these extra spots are due to multiple scattering. The most prominent set of multiple scattering spots is the quadruplet enclosed by the rectangle. During our in-situ x-ray experiments, we searched *extensively* and *carefully* in this area of reciprocal space for the quadruplet, but did not find any diffraction from the Bi monolayer. Thus, since the in-situ and ex-situ Bi structures are the same, the quadruplet observed in the LEED experiment must be due to multiple scattering.

We now show how the multiple scattering spots indicated in Figure 6(a) arise from double diffraction between the Bi monolayer and the Ag substrate. Figure 6(b) demonstrates this explicitly for the quadruplet enclosed by the rectangle in Figure 6(a): The heavy solid line is an Ag surface reciprocal lattice vector, while the thinner solid lines



are Bi reciprocal lattice vectors. Double diffraction occurs at positions given by the sum of all the Ag and Bi reciprocal lattice vectors. Figure 6(b) shows that this sum produces two of the four members of the quadruplet; the other two members are obtained by double diffraction from symmetry equivalent Ag and Bi reciprocal lattice vectors. (These are not shown but obtained by a simple reflection of the Figure about the horizontal axis). As Figure 6(b) also suggests, one is tempted to expect diffraction at the position indicated by the small open circle. However, this is at the same position as the Bi(01) diffraction spot, which is kinematically forbidden because of the glide plane in the Bi structure. For a normal incidence LEED experiment, this spot is also *dynamically* forbidden, as shown theoretically by Holland and Woodruff<sup>29</sup> and demonstrated experimentally.<sup>30</sup> Thus, it is not observed in the LEED experiment of ILSH.<sup>5</sup> If the LEED experiment was performed with the incident electron beam at some off-normal incidence angles, then this multiple scattering spot would be seen.<sup>29</sup>

Figure 6(c) shows all the multiple scattering spots generated by double diffraction between the Ag substrate and the Bi monolayer. As is clearly seen, double diffraction successfully explains the multiple scattering spots enclosed by the triangles in Figure 6(a), and in addition, predicts two sets of spots near the origin (marked by arrows). These spots (and the other spots represented by filled squares) are not seen in the 47eV LEED pattern from the ex-situ experiment;<sup>5</sup> this is presumably due to the spots having a small intensity at 47eV, although a dynamical calculation is necessary to confirm this. The sets of spots marked by arrows are, however, observed in LEED measurements (at 37eV) of vapor deposited Bi on Au(111),<sup>31</sup> which we believe has the same rectangular structure as Bi/Ag(111), as described below.

For incommensurate adsorbed layers, double diffraction between the monolayer and the substrate has often been observed in LEED experiments.<sup>32-37</sup> For example, the LEED patterns of vapor deposited Pb on Ag(111) and Cu(111) clearly show double diffraction spots that are observed at the sum of substrate and adsorbed monolayer reciprocal lattice vectors.<sup>32</sup> Many inert gases adsorbed on graphite form layers that are

incommensurate with the graphite, and for these systems, double diffraction is always observed in LEED.<sup>33, 34</sup> Similarly, double diffraction also appears in LEED experiments on the uniaxially commensurate phase of Xe/Cu(110).<sup>36</sup>

Our previous results show that the in-situ structure of UPD monolayers of Tl and Pb on Au(111) and Ag(111) is the same as the vapor deposited metal monolayers - namely, incommensurate, rotated hexagonal overlayers.<sup>9, 14, 22</sup> Unfortunately, we are not aware of any measurements of vapor deposited Bi/Ag(111). There is, however, a report of vapor deposited Bi/Au(111)<sup>31</sup> and the LEED pattern for this system (obtained at 37eV) is remarkably similar to that shown in Figures 6(a) and (c). This similarity strongly suggests that the monolayer of vapor deposited Bi on Au(111) forms a rectangular structure, similar to UPD Bi/Ag(111). In addition, the LEED pattern for Bi/Au(111)<sup>31</sup> clearly shows the two sets of six spots marked with small arrows in Figure 6(c). The observation of these spots at the positions predicted by double scattering further supports our conclusion that Bi on Ag(111) and Au(111) form centered rectangular structures. It would be interesting to see a study of vapor deposited Bi/Ag(111).

In summary, we are confident that the in-situ and ex-situ structures for Bi/Ag(111) are both uniaxially commensurate rectangular structures. This is intuitively appealing, since the in-situ rectangular structure is considerably simpler than the  $2\sqrt{3} \times 2\sqrt{3} - R30^\circ$ , anti-phase domain structure proposed from the ex-situ measurements.<sup>5</sup> In addition, the coverage calculated from our structure (see Figure 4) is in excellent agreement with the total charge measured during the deposition of Bi, as determined by us (see Figure 1) and as reported in the literature.<sup>15, 16</sup> While the structure of Bi/Ag(111) was not altered in the ex-situ experiments, UPD layers of Tl and Pb on Ag(111) are dramatically changed in similar experiments.<sup>4, 5</sup> During removal of the electrode from the electrolyte, loss of potential control, and transfer into UHV, Tl and Pb UPD layers are oxidized and their structure changes. Thus, emersion can certainly cause changes in adsorbed layers. However, our findings suggest that in the absence of

chemical reaction, an alteration of UPD layers on emersion is not inevitable and the solid/liquid interfacial structure may be preserved in ex-situ emersion experiments.

### *V. Summary and Conclusions*

We have described in-situ surface x-ray scattering measurements of electrochemically deposited Bi monolayers on Ag(111). The Bi monolayer adopts an unusual structure: a rectangular lattice that is uniaxially commensurate with the hexagonal Ag(111) surface along the Ag  $[\bar{2}11]$  direction. There are two Bi atoms per unit cell with one displaced from the centered-rectangular position by about  $0.25\text{\AA}$  along the commensurate direction. This distortion indicates a tendency of the Bi adatoms to form zig-zag rows running along the incommensurate direction (Ag  $[01\bar{1}]$ ). It shortens two of the Bi-Bi near-neighbor distances while lengthening two others and probably reflects the tendency toward covalent bonding in Bi. As the applied potential decreases, the Bi monolayer compresses uniaxially along the incommensurate direction (Ag  $[01\bar{1}]$ ), preserving the uniaxially commensurate structure. The 2D compressibility of the Bi monolayer was measured as  $\kappa_{2D} = 0.75\text{\AA}^2/\text{eV}$ , which is comparable to our results for Tl and Pb monolayers on Ag(111) and Au(111)<sup>6, 9, 21</sup> and is in reasonable agreement with a model calculation. We also found that the presence or absence of  $\text{Cl}^-$  ions in concentrations up to  $0.35\text{mM}$  does not affect the structure or compressibility.

The results of these surface x-ray scattering measurements are very important: first, they allow a direct determination of the in-situ structure of UPD Bi/Ag(111), and second, they permit, *for the same system*, the first direct comparison between an in-situ structure and ex-situ measurements on emersed electrodes, where the monolayer structure was determined following transfer to UHV.<sup>5</sup> Although the in-situ uniaxial commensurate, distorted rectangular structure is quite different from the structure proposed in the ex-situ experiments, we believe that the in-situ and ex-situ structures are, in fact, the same. When double-diffraction is considered, the in-situ structure completely explains the published ex-situ LEED data;<sup>5</sup> in contrast, the proposed

$2\sqrt{3} \times 2\sqrt{3} - R30^\circ$ , anti-phase domain structure is inconsistent with our (kinematic) surface x-ray scattering data.

This comparison demonstrates that, at least for the case of Bi/Ag(111), the ex-situ emersion experiments can preserve the spatial arrangement of the adsorbed atoms. Although the emersion technique can produce drastic changes in the in-situ interfacial structure,<sup>4, 5</sup> the preservation of the interfacial structure in this one case offers the possibility (and hope) that emersion need not always alter the interfacial structure. In-situ surface x-ray scattering experiments on additional systems are clearly needed to understand when and why the interfacial structure is preserved.

Our experiments also clearly demonstrate a great advantage of x-ray diffraction compared to electron diffraction. X-rays are weakly interacting and (for surfaces) the x-ray diffraction pattern can be analyzed kinematically, without considering multiple scattering. In contrast, electrons are very strongly interacting, and multiple scattering must be properly taken into account during data analysis. Although the influence of multiple scattering on LEED intensities is widely appreciated, it is important to note that for incommensurate adsorbed layers, multiple scattering leads to additional LEED spots that are not predicted based on kinematic considerations. In these cases, great care is needed to ensure proper interpretation of LEED patterns.

### *Acknowledgments*

We thank Jean Jordan-Sweet and Brian Stephenson for their assistance with beam line X20C. We also thank Doug Frank and Art Hubbard for useful discussions and for supplying us with their ex-situ LEED data. This work was partially supported by the Office of Naval Research. It was performed at the National Synchrotron Light Source (NSLS), which is supported by the U.S. Department of Energy, Division of Material Sciences and Division of Chemical Sciences (DOE contract number DE-AC02-76CH00016).

## References

- <sup>1</sup> A.T. Hubbard, *Acc. Chem. Res.* **13**, 177 (1980).
- <sup>2</sup> P.N. Ross, *Surface Sci.* **102**, 463 (1981).
- <sup>3</sup> E. Yeager, *J. Electroanal. Chem.* **128**, 463 (1981).
- <sup>4</sup> M.E. Hanson and E. Yeager, in *Electrochemical Surface Science*, edited by M.P. Soriaga, (American Chemical Society, 1988), p. 141.
- <sup>5</sup> L. Laguren-Davidson, F. Lu, G.N. Salaita, and A.T. Hubbard, *Langmuir* **4**, 224 (1988).
- <sup>6</sup> M.F. Toney and O.R. Melroy, in *In-Situ Studies of Electrochemical Interfaces*, edited by H.D. Abruna, (VCH Verlag Chemical, 1990).
- <sup>7</sup> M.G. Samant, M.F. Toney, G.L. Borges, L. Blum, and O.R. Melroy, *Surf. Sci.* **193**, L29 (1988).
- <sup>8</sup> M.G. Samant, M.F. Toney, G.L. Borges, L. Blum, and O.R. Melroy, *J. Phys. Chem.* **92**, 220 (1988).
- <sup>9</sup> O.R. Melroy, M.F. Toney, G.L. Borges, M.G. Samant, J.B. Kortright, P.N. Ross, and L. Blum, *Phys. Rev. B* **38**, 10962 (1988).
- <sup>10</sup> J.G. Gordon, O.R. Melroy, G.L. Borges, D.E. Reisner, P. Chandrasekhar, H. Abruna, and L. Blum, *J. Electroanal. Chem.* **210**, 311 (1986).
- <sup>11</sup> E.D. Specht, A. Mak, C. Peters, M. Sutton, R.J. Birgeneau, K.L. D'Amico, D.E. Moncton, S.E. Nagler, and P.M. Horn, *Z. Phys. B* **69**, 347 (1987).
- <sup>12</sup> G.B. Stephenson, *Nucl. Instr. Meth.* **A266**, 447 (1988).
- <sup>13</sup> W.R. Busing and H.A. Levy, *Acta Cryst.* **22**, 457 (1967).
- <sup>14</sup> M.F. Toney, J.G. Gordon, L.S. Kau, G. Borges, O.R. Melroy, M.G. Samant, D.G. Wiesler, D. Yee, and L.B. Sorensen, *Phys. Rev. B*, in press, 1990.
- <sup>15</sup> J.W. Schultze and K.R. Brenske, *J. Electroanal. Chem.* **137**, 331 (1982).
- <sup>16</sup> J.W. Schultze, D. Dickertmann, and F.D. Koppitz, *Faraday Symp.* **12**, 167 (1977).
- <sup>17</sup> D. Kolb, M. Przasnyski, and H. Gerischer, *J. Electroanal. Chem.* **54**, 25 (1974).
- <sup>18</sup> D.M. Kolb, in *Advances in Electrochemistry and Electrochemical Engineering*, edited by H. Gerischer and C.W. Tobias, (Wiley, New York, 1978), Vol. 11, p. 125.

- <sup>19</sup> I.K. Robinson, Phys. Rev. B 33, 3830 (1986).
- <sup>20</sup> M.F. Toney, J.G. Gordon, G. Borges, D.G. Wiesler, D. Yee, and L.B. Sorensen, unpublished, 1991
- <sup>21</sup> M.F. Toney, J.G. Gordon, L.S. Kau, G. Borges, O.R. Melroy, M.G. Samant, D.G. Wiesler, D. Yee, and L.B. Sorensen, unpublished, 1990
- <sup>22</sup> M.F. Toney and O.R. Melroy, in *Synchrotron Radiation in Materials Research, MRS Symp. Proc., Vol. 143*, edited by R. Clarke, (Materials Research Society, 1989), p. 37.
- <sup>23</sup> C.G. Shaw and S.C. Fain, Surf. Sci. 83, 1 (1979).
- <sup>24</sup> C.G. Shaw and S.C. Fain, Surf. Sci. 91, L1 (1980).
- <sup>25</sup> L.W. Bruch and J.M. Phillips, Surf. Sci. 91, 1 (1980).
- <sup>26</sup> J. Unguris, L.W. Bruch, E.R. Moog, and M.B. Webb, Surf. Sci. 109, 522 (1981).
- <sup>27</sup> J.G. Dash, *Films on Solid Surfaces*, (Academic Press, New York, 1975).
- <sup>28</sup> D. Frank and A.T. Hubbard, private communication, 1989
- <sup>29</sup> B.W. Holland and D.P. Woodruff, Surface Sci. 36, 488 (1973).
- <sup>30</sup> R.D. Diehl, M.F. Toney, and S.C. Fain, Phys. Rev. Lett. 48, 177 (1982).
- <sup>31</sup> A. Sepulveda and G.E. Rhead, Surface Sci. 49, 669 (1975).
- <sup>32</sup> K.J. Rawlings, M.J. Gibson, and P.J. Dobson, J. Phys. D 11, 2059 (1978).
- <sup>33</sup> M.D. Chinn and S.C. Fain, Phys. Rev. Lett. 39, 146 (1977).
- <sup>34</sup> C.G. Shaw, S.C. Fain, and M.D. Chinn, Phys. Rev. Lett. 41, 955 (1978).
- <sup>35</sup> J. Unguris, L.W. Bruch, E.R. Moog, and M.B. Webb, Surf. Sci. 87, 415 (1979).
- <sup>36</sup> A. Glachant, M. Jaubert, M. Bienfait, and G. Boato, Surface Sci. 115, 219 (1981).
- <sup>37</sup> D.L. Doering and S. Semancik, Surface Sci. 129, 177 (1983).

## Figure Captions

Figure 1. Measured cyclic voltammograms for the UPD of Bi on Ag(111). The voltammogram is obtained by linearly sweeping the electrode potential in the negative direction from a suitable positive potential. The potentials were measured relative to the Ag/AgCl (3M KCl) reference electrode. (a) Deposition of Bi in chloride-free solution (0.1M HClO<sub>4</sub> containing 2.5mM Bi<sub>2</sub>O<sub>3</sub>). (b) Deposition of Bi in chloride-containing solution (0.1M HClO<sub>4</sub> containing 2.5mM Bi<sub>2</sub>O<sub>3</sub> and 0.35mM NaCl). The total charge passed during deposition is 450-480  $\mu\text{C}/\text{cm}^2$  (from the area under voltammogram).

Figure 2. In-situ surface x-ray diffraction pattern for Bi/Ag(111). (a) The pattern that would be observed for a single domain of the rectangular Bi monolayer. The size of the filled circles indicates the approximate observed intensity for each diffraction peak, while the open squares indicate reflections we did not measure (because of lack of time or because the Bi peak was obscured by a mica peak). The Bi (03) peaks, indicated by the crosses, were too weak to be measured. The Ag surface peaks are shown by open circles; note that the Bi(20) peaks overlap two of the Ag surface peaks. The dashed line shows an example of an  $h$  scan. (b) The observed diffraction pattern, which is the incoherent superposition of all three domains present on the surface. All peaks are indicated by filled circles. This pattern is shown on the same scale as Figure 6, so the x-ray and LEED patterns can be directly compared.

Figure 3. In-situ x-ray diffraction scans from a Bi monolayer on Ag(111). The perpendicular component of the scattering vector was fixed at  $Q_z = 0.13\text{\AA}^{-1}$  and the layer was deposited at 60mV from the chloride-containing electrolyte. The ordinate is the number of counts received by the detector normalized by the monitor counts. (a) The Bi (11) peak. (b) The Bi (31) peak. (c) The Bi (30) peak. (d) A scan through the expected position for the Bi (03) peak (which is marked with the arrow). The dashed line shows the background x-ray scattering, which was obtained at 250mV, where the monolayer is completely desorbed. It is uniformly smaller (by 2%) than the data at

60mV (circles), because the electrolyte thickness changed slightly during stripping of the monolayer. Since the large peak at about  $4.16\text{\AA}^{-1}$  is present at both potentials, it is caused by scattering from the mica substrate or the polypropylene film covering the electrode. The inset shows the difference between the data at 60mV and at 250mV, demonstrating there is no observable intensity in the (03) peak. A typical error bar is shown.

Figure 4. In-situ structure of Bi/Ag(111). The open circles represent the surface atoms of the Ag substrate (with hexagonal symmetry) and the shaded circles represent the Bi adatoms. The relative sizes of these circles correspond to the near neighbor spacing of bulk Ag ( $2.89\text{\AA}$ ) and bulk Bi ( $3.07\text{\AA}$ ). The distortion of the centered Bi adatom is shown as  $0.25\text{\AA}$ , and for clarity, the Bi[10] rows are shown atop the Ag  $[01\bar{1}]$  rows, although we have not yet determined the epitaxy. The Bi monolayer is commensurate in the  $a$  direction, ( $a = 5.005\text{\AA} = \sqrt{3}$  times Ag nearest-neighbor distance), but is incommensurate in the  $b$  direction ( $b = 4.484\text{\AA} - 4.566\text{\AA}$ ).

Figure 5. Dependence of the Bi monolayer lattice constants on the applied potential,  $V$ . The triangles and circles are for chloride-free and chloride-containing electrolytes, respectively. (a) The lattice constant  $a$ . The average value is  $a = 5.005 \pm 0.001\text{\AA}$  (standard deviation of the mean), demonstrating the Bi monolayer is uniaxially commensurate with the Ag surface. (b) The lattice constant  $b$ . The line is a linear least-squares fit to the data and has a slope  $db/dV = -0.9\text{\AA}/V$ .

Figure 6. Low-energy electron diffraction patterns for Bi/Ag(111). The Ag diffraction spots are indicated by open circles. (a) Trace of the LEED pattern as determined by LLSH in their ex-situ experiment (an electron energy of 47eV at normal incidence).<sup>5, 28</sup> There is some distortion in this pattern caused by distortions in the LEED screen. The observed intensities are roughly indicated by the spot sizes. The rectangles and triangles enclose diffraction spots that are not kinematically allowed for the in-situ rectangular structure. (b) The double-scattering origin of the quadruplet enclosed by the



rectangle in (a). The heavy solid line is an Ag reciprocal lattice vector and the thinner solid lines are Bi reciprocal lattice vectors. For each of the three domains, double diffraction occurs at all positions given by the sum of Ag and Bi reciprocal lattice vectors. The origin of two of the four members of the quadruplet is illustrated. (c) The predicted LEED pattern for the in-situ rectangular structure including double-diffraction spots. The filled circles show the single-scattering (or kinematic) spots, while the squares show spots due to double scattering. The open squares indicate spots (or symmetry equivalent spots) that were observed by LLSII at 47eV.<sup>5</sup> The filled squares represent spots that will be observed at different electron energies and the arrows mark spots that were observed at 37eV for vapor deposited Bi/Au(111),<sup>31</sup> which we believe has the same structure as Bi/Ag(111).

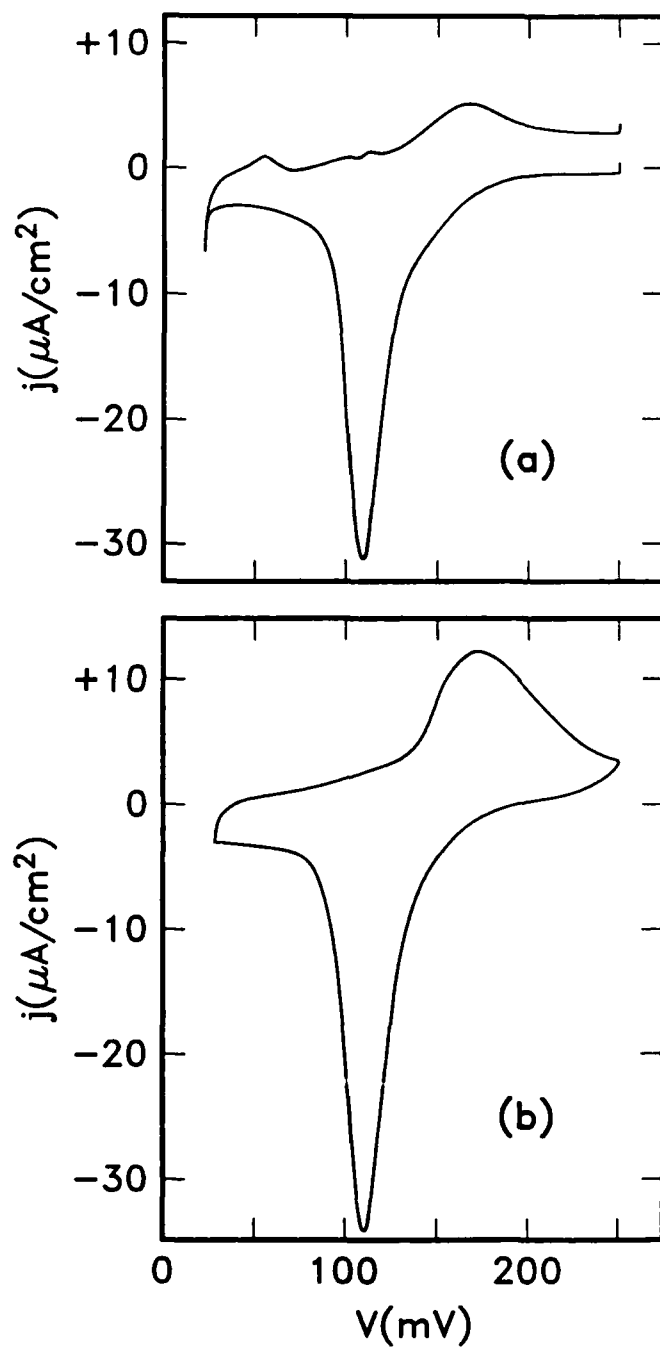


Figure 1

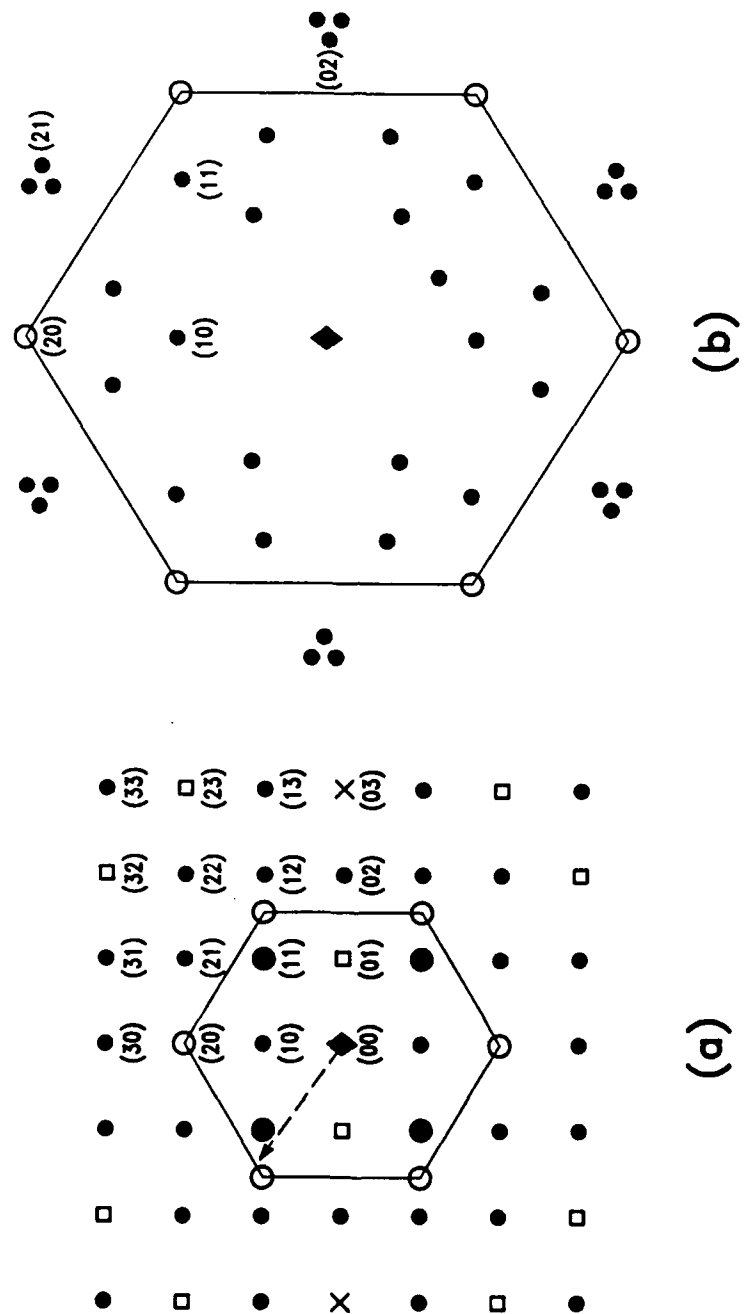


Figure 2

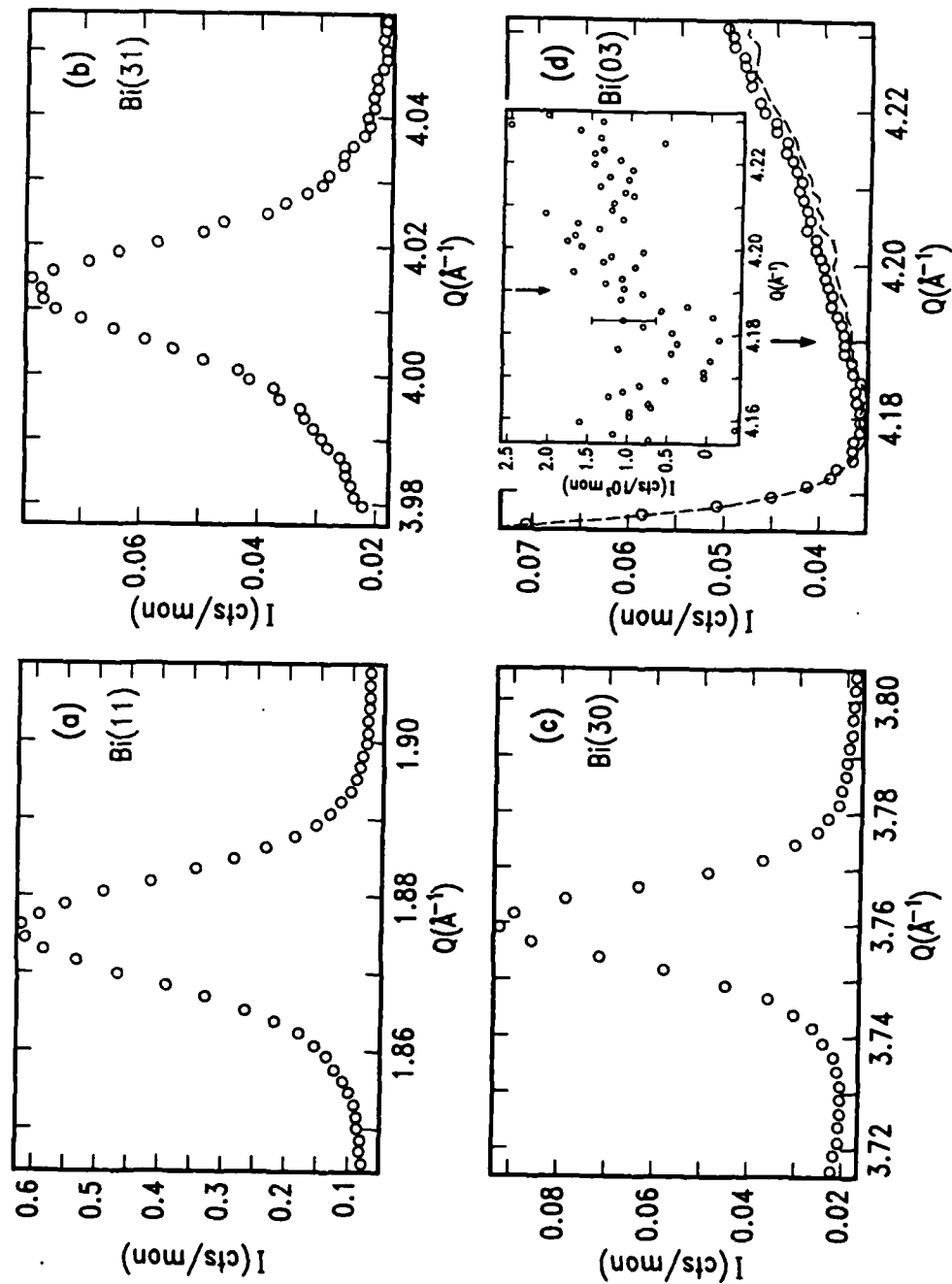


Figure 3

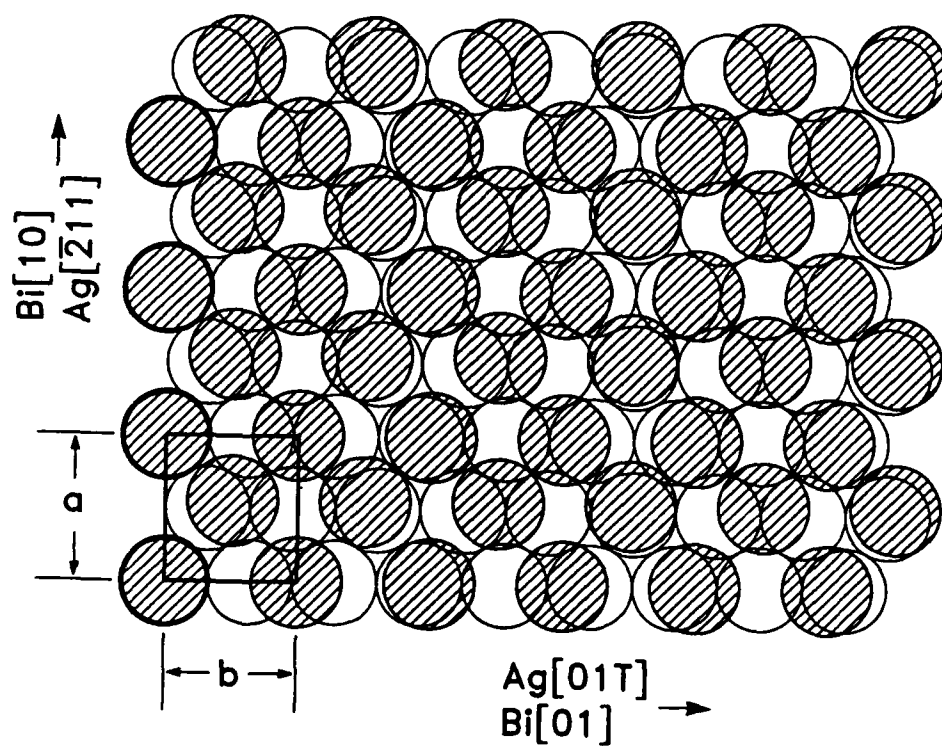


Figure 4

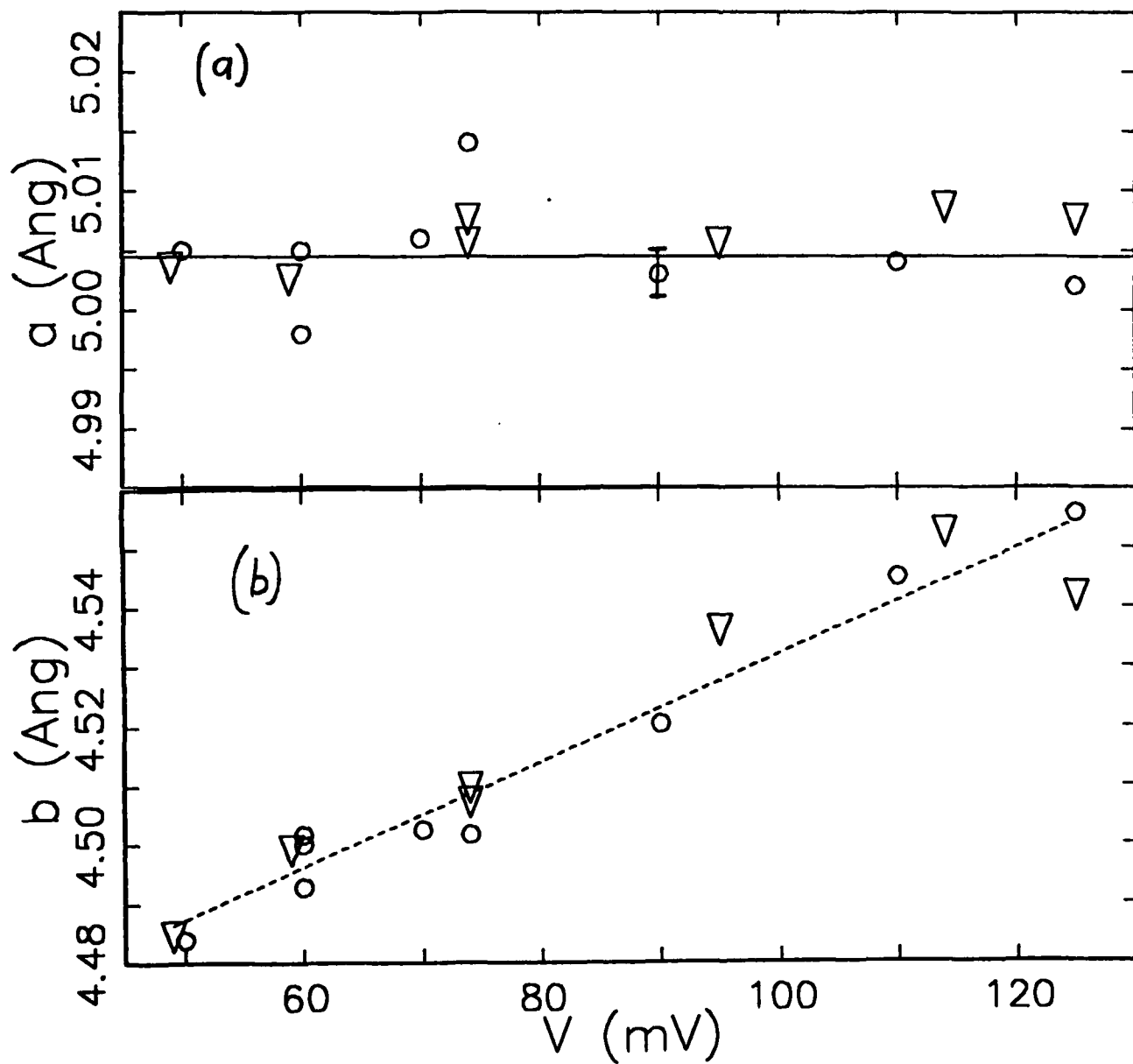


Figure 5

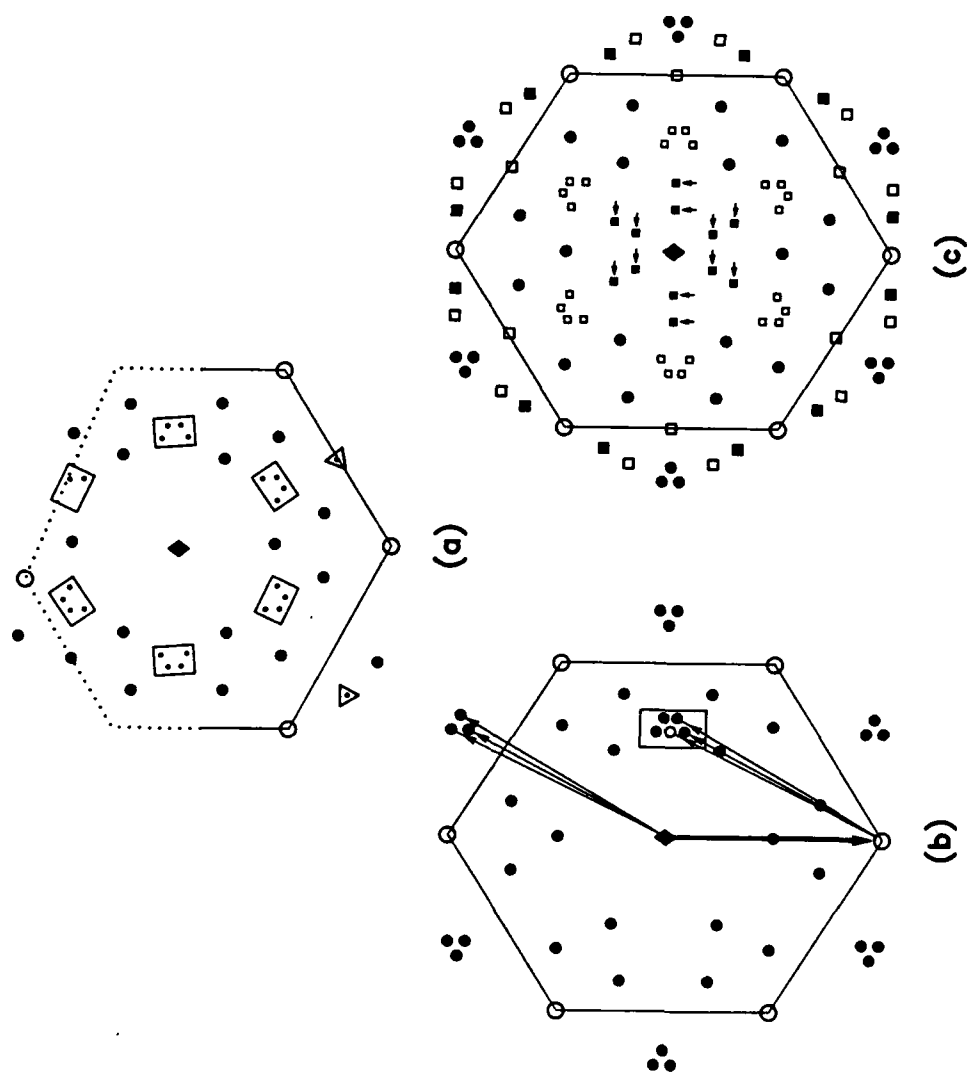


Figure 6